

PHOTOSENSITIVITY AND NOISE OF ULTRAFAST InGaAs/InP AVALANCHE PHOTODIODES

J. Matukas^a, V. Palenskis^a, S. Pralgauskaitė^a, R. Gadonas^b, R. Purlys^c, A. Čiburys^b,
and A. Vizbaras^a

^a *Radiophysics Department, Faculty of Physics, Vilnius University, Saulėtekio 9, LT-10222 Vilnius, Lithuania*

E-mail: jonas.matukas@ff.vu.lt, vilius.palenskis@ff.vu.lt, sandra.pralgauskaite@ff.vu.lt, augustinas.vizbaras@ff.vu.lt

^b *Department of Quantum Electronics, Faculty of Physics, Vilnius University, Saulėtekio 9, LT-10222 Vilnius, Lithuania*

E-mail: roaldas.gadonas@ff.vu.lt, arunas.ciburys@ff.vu.lt

^c *Department of Solid State Electronics, Faculty of Physics, Vilnius University, Saulėtekio 9, LT-10222 Vilnius, Lithuania*

E-mail: romaldas.purlys@ff.vu.lt

Received 22 November 2006

A detailed investigation of photosensitivity and noise characteristics of ultrafast InGaAs/InP avalanche photodiodes with separate absorption, grading, charge, and multiplication regions was carried out. Carrier multiplication and noise factors were evaluated, and influence of the ionizing radiation to the avalanche photodiode operation quality was investigated. Carrier multiplication and noise factors can be correctly evaluated only if input light beam is well focused to the active photodiode area since the peripheral area is quite sensitive to the infrared radiation, too. Photodiode irradiation by X-ray radiation can lower the defect density in the device structure or create new defects depending on radiation power and duration. Noise characteristics not only clarify fundamental physical processes in avalanche photodiode structure, but also indicate the presence and appearance of defects in the devices.

Keywords: avalanche photodiode, multiplication, noise, photosensitivity

PACS: 85.60.Dw, 07.50.Hp

1. Introduction

The InGaAs/InP-based avalanche photodiodes (APDs) with separate absorption, grading, charge, and multiplication (SAGCM) regions provide wide dynamical range, high linearity, and saturation power up to the 10 Gbit/s data transmission speed [1, 2].

Photosensitivity of the light receiving devices is one of the main parameters that determine the maximum distance between signal regenerators in optical data transmission systems. On the one hand, excess noise lowers photodetector sensitivity, on the other hand, low noise spectroscopy is well known as an especially sensitive method to probe defects within the semiconductor structures, assess their quality, and predict semiconductor device lifetime [3–5]. Therefore, the noise characteristics investigation is very important for the higher quality APD design and fabrication.

There are very few published results on low-frequency noise in InGaAsP/InP-based APDs [6, 7], and the measurements are carried out in a narrow frequency range (1–100 Hz). In this frequency range it is difficult

to distinguish between the generation-recombination and shot noises. Multiplication shot noise is conditioned by device material and structure (it is not related with defects) and can be described by McIntyre relation [8, 9]. McIntyre relation considers that electron and hole ionization factors depend only on the local electrical field. However, multiplication layer of ultrafast APDs is very narrow, so, multiplication factor can be influenced not only by the local processes [10, 11].

Excess multiplication noise is characterized by noise factor that increases with multiplication increasing. Thus, multiplication noise characteristic analysis is important in optimizing photodiode design. Defects and impurities, alternation of multiplication layer thickness lead to the multiplication factor changes across the photodiode surface [12, 13]. The larger noise factor is observed in devices with non-uniform multiplication factor distribution [9].

In this work, a detailed study of ultrafast InGaAsP/InP avalanche photodiodes photosensitivity and noise characteristics is presented.

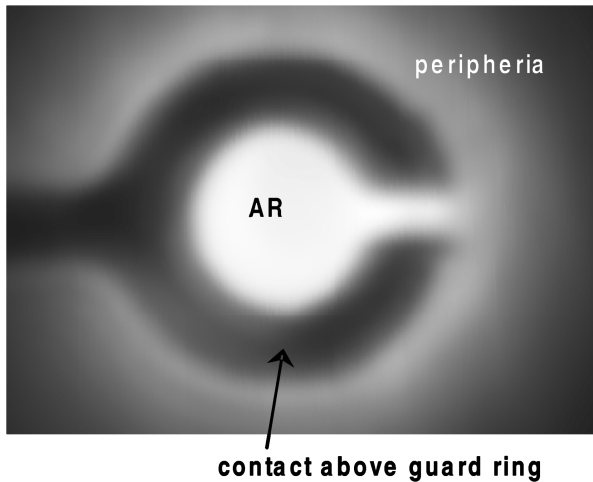


Fig. 1. The APD surface view (AR is active region) obtained by scanning photocurrent distribution.

2. Investigated devices and measurement technique

The investigated devices were InGaAs/InP-based avalanche photodiodes with separate absorption, grading, charge, and multiplication regions used for 10 Gbit/s fibre-optic communication applications. The APD structures [14] were grown in a single reactor growth cycle by MOCVD. Product of amplification factor and bandwidth for the investigated devices exceeds 100 GHz.

The device active region area is $20\ \mu\text{m}$ in diameter and it is surrounded by a guard ring (Fig. 1). Active surface is coated with antireflection SiN_x layer.

Photocurrent–voltage characteristic, terminal voltage, and current fluctuation dependences on reverse bias were measured. For the noise investigation APD was illuminated by a halogen bulb (HB) with silicon filter (in order to eliminate visible light and leave infrared one). HB illuminates the whole APD surface: both the active region in the centre and the peripheral area outside the metal contact. There is no possibility to focus incoherent HB light, but its emitted light is distinguished by very low $1/f$ noise. Thus HB is suitable as a light source for the noise measurement over whole APD surface. Noise characteristics were investigated in the frequency range from 20 Hz to 20 kHz.

For the photosensitivity distribution measurement a semiconductor laser emitting at $1.55\ \mu\text{m}$ was used as a light source. Laser light beam can be well focused to a spot with diameter in the range of $2\text{--}3\ \mu\text{m}$ and individual parts of the active and peripheral regions can be illuminated step-by-step.

APD photosensitivity and noise characteristics measurement circuit is presented in Fig. 2. For the pho-

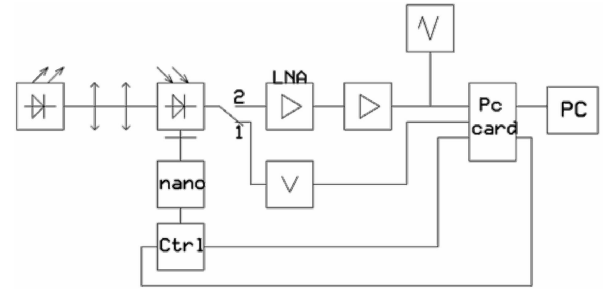


Fig. 2. APD photocurrent and noise measurement circuit (LNA is a low noise amplifier, nano is a micromanipulator NanoCube© P-611.3S, Ctrl is a controller E-664.3S, Pc card is a National Instruments™ PCI card AT-M10-16E-10).

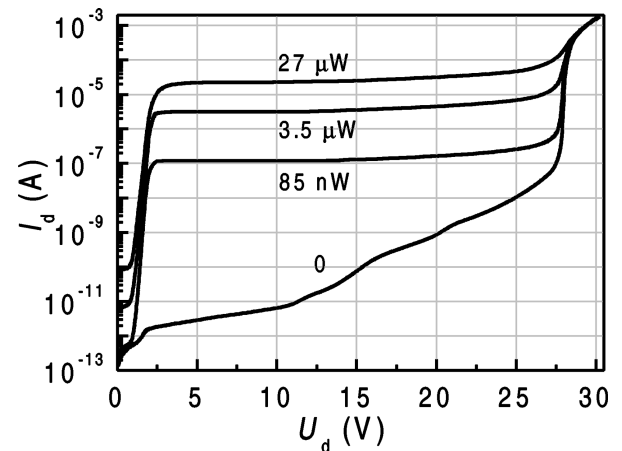


Fig. 3. Typical APD dark current (0) and photocurrent (85 nW, $3.5\ \mu\text{W}$, $27\ \mu\text{W}$) dependences on reverse bias at different input light power (illuminated with HB).

tocurrent distribution in different active surface areas the micromanipulator Nanocube© P-611.3S and controller E-664.3S with a scanning area of $100 \times 100\ \mu\text{m}^2$ were used. In the case when the switch is in position 1, the photovoltage is measured, whereas in the position 2 the noise characteristics are measured.

3. Results and discussion

3.1. APD photocurrent

Current–voltage characteristics of investigated avalanche photodiode, measured when the whole photodiode surface (active and peripheral regions) is illuminated by a halogen bulb, are presented in Fig. 3. A dark current does not exceed 10 pA at reverse bias less than 10 V. Photocurrent saturates at a voltage of 3 V (that corresponds to the guard ring punch-through voltage, when the space charge region reaches the guard ring interface) and stays almost constant up to 13 V (that is punch-through voltage, when the space charge region

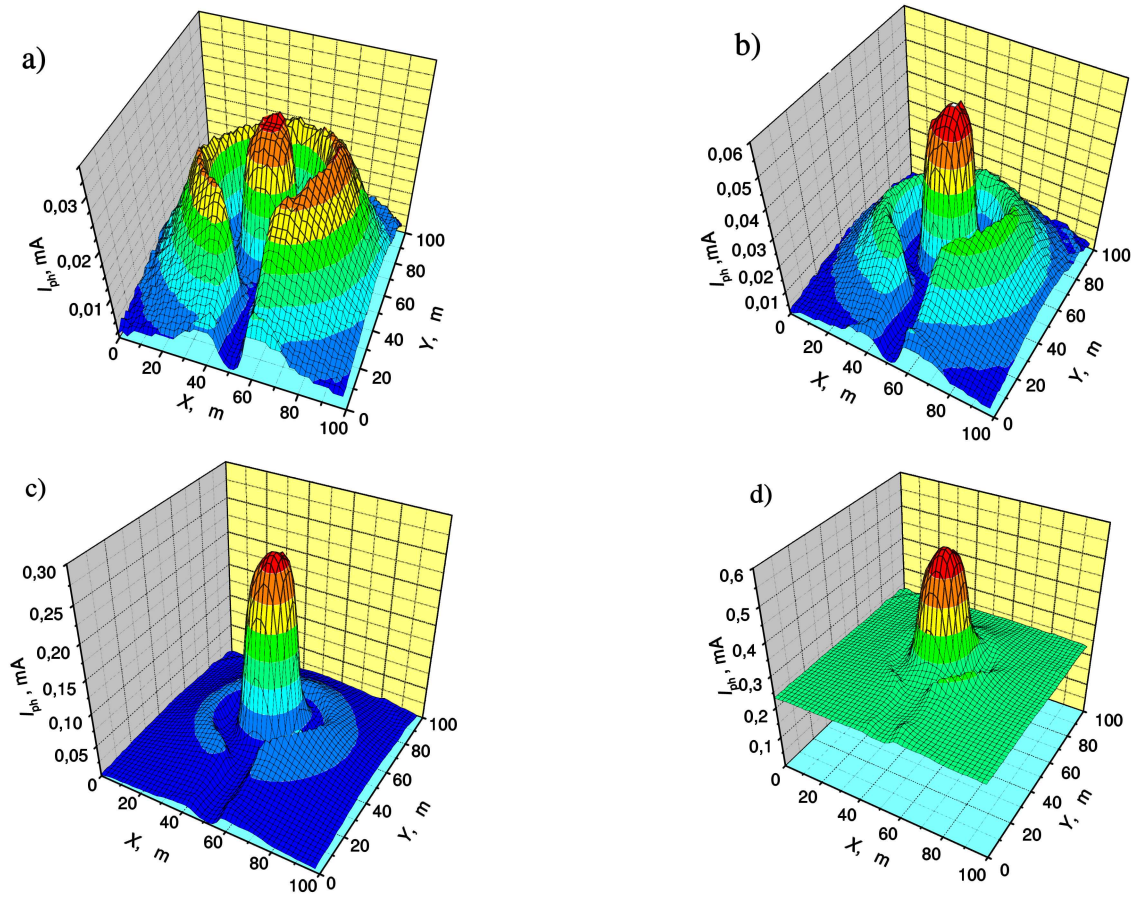


Fig. 4. Photocurrent distribution in active and peripheral regions at different reverse bias: (a) 7 V, (b) 15 V, (c) 27 V, (d) 29 V (illuminated with semiconductor laser by using NanoCube scanning).

completely spans the light absorption layer and is sufficient for impact ionization; Fig. 3). In this region the carrier multiplication factor is equal to one. At further reverse voltage increasing the multiplication factor increases up to 10 at low input light power (< 85 nW).

Using a semiconductor laser as focused infrared light source and micromanipulator, the photocurrent (photosensitivity) distribution in the active and peripheral APD regions was investigated (Fig. 4). The results have shown that peripheral region is sensitive to the infrared radiation and, if photodiode is illuminated by incoherent light that cannot be focused only in the active region, photocurrent is a sum of both active area photocurrent and peripheral area photocurrent.

At reverse bias lower punch-through voltage (about 13 V) the photocurrent is low both in the active and peripheral regions, but the photocurrent in active region is slightly larger than photocurrent maximum in peripheral region (graph (a) in Fig. 4). With reverse voltage increasing, the photocurrent in the active region quickly increases due to the carrier multiplication, while the increase of photocurrent in the peripheral area is rather

slow (graphs (b) and (c) in Fig. 4). At deep avalanche breakdown (above 28 V for the sample in Fig. 4) a dark current strongly increases, and a “floating” background represents the dark current level (graph (d) in Fig. 4). Therefore, the measurement results obtained by illuminating photodiode surface with incoherent light (when both active and peripheral surfaces are illuminated) are not suitable for the carrier multiplication factor and the multiplication shot noise factor evaluation, as photocurrent dependences on reverse bias in active and peripheral regions are different. For these purposes a strongly focused light source has to be used (the diameter of the laser beam must be smaller than dimensions of the active area).

Laser light beam was strongly focused within the active area or only to the periphery (the light spot diameter in both cases was kept constant). The photocurrent dependences on reverse bias measured in this way are presented in Fig. 5. The photocurrent in the active area abruptly increases due to carrier multiplication process, when reverse bias exceeds the punch-through voltage.

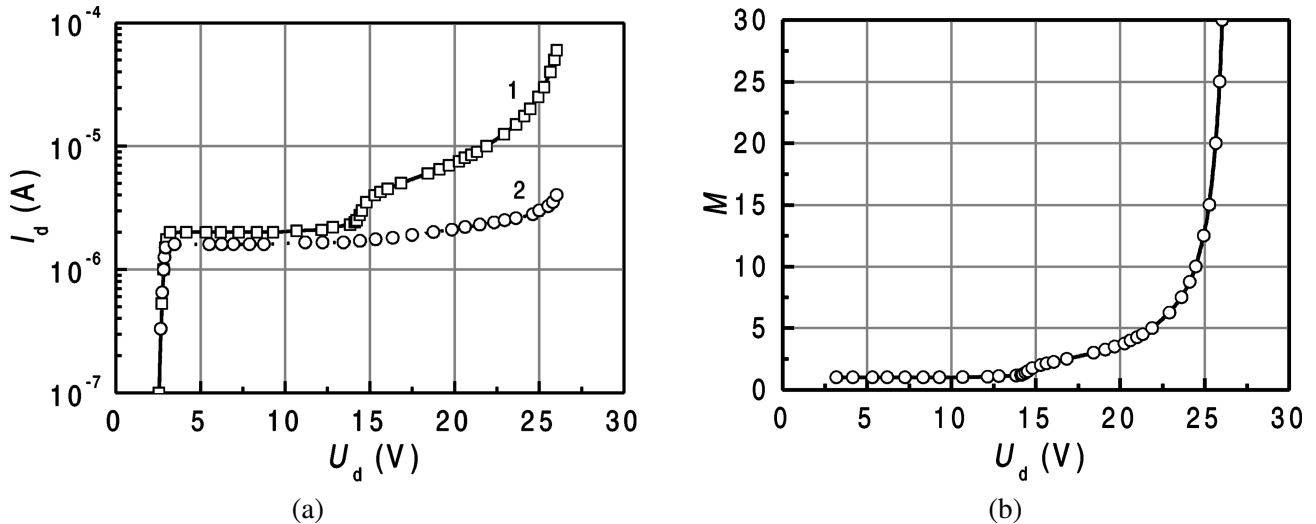


Fig. 5. (a) Photocurrent in the active (line 1) and peripheral (line 2) APD regions and (b) the carrier multiplication factor dependences in the active area on reverse bias (illuminated with semiconductor laser).

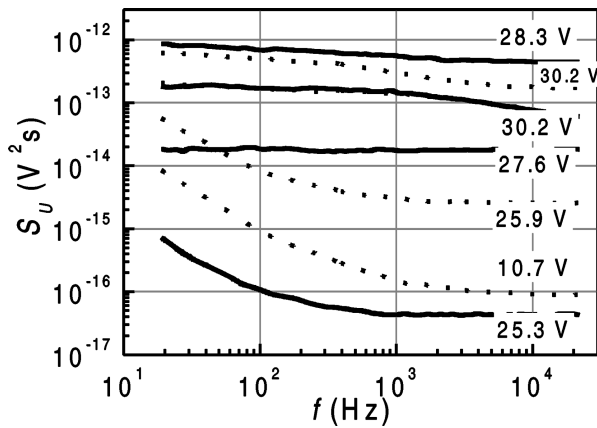


Fig. 6. Typical APD voltage noise spectra at different input light power (solid line at 85 nW, dot line at 27 μ W) and at various reverse voltages (illuminated by HB).

The photocurrent multiplication factor in the peripheral area is much smaller.

Carrier multiplication factor at bias lower punch-through voltage does not depend on reverse bias and is approximately equal to unity (graph (b) in Fig. 5). At avalanche breakdown region the carrier multiplication factor exceeds the value of 30.

3.2. APD noise characteristics

Noise spectra of avalanche photodiodes mainly consist of shot noise, generation-recombination fluctuations, and $1/f$ type noise. At reverse bias below punch-through voltage (12–15 V), i. e. while there is no carrier multiplication, the noise level of the investigated APDs is low and is determined by the shot noise and the non-intensive $1/f$ type noise (Fig. 6). At reverse voltage below 25 V, the white noise level increases with light

increasing due to the increasing photon flow. At deep breakdown voltages (above 30 V) large noise is determined by dark current. And this noise decreases with light power increasing. Low $1/f$ type noise level indicates a good quality of the investigated APDs. Shot noise abruptly increases as avalanche breakdown process takes place. Still larger increase is observed in generation-recombination noise, which is determined by carrier recombination at multiplication and absorption layer interfaces. Relaxation times of the observed generation-recombination fluctuations vary from several tens of microseconds to several tens of milliseconds. So, the noise investigation in frequency range below 100 Hz in many cases does not give the correct multiplication shot noise factor values because shot noise can be masked by generation-recombination one.

In Fig. 7, there are presented APD voltage noise spectra, when active and peripheral regions are illuminated separately. When only the active region is illuminated, the shot noise exceeds low frequency generation-recombination noise only at frequencies above 20 kHz (noise level for multiplication shot noise was evaluated at 30 kHz). If only peripheral region is illuminated, the photocurrent is lower comparing with the one of active area and, consequently, shot noise is rather low (Fig. 7).

It was observed that the $1/f$ type noise level, when both the active and the peripheral areas are illuminated by a halogen lamp, is noticeably lower than that when only the active area is illuminated by laser. These results can be explained by the intensive recombination processes at the active region edges.

When avalanche carrier multiplication takes place, excess white multiplication noise determined by the

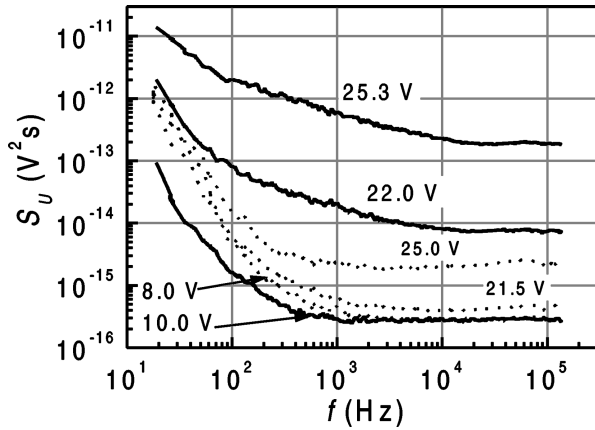


Fig. 7. APD voltage noise spectra at different reverse bias: solid line for the active region, dot line for the peripheral region (illuminated with semiconductor laser by using constant beam spot).

random ionization events is additionally present. This excess multiplication shot noise is defined by the noise factor F multiplied by the shot noise spectral density:

$$S_i = 2qI_{act0}M^2F, \quad (1)$$

where S_i is the multiplication shot noise spectral density, q is the electron charge, I_{act0} is the initial photocurrent, when carrier multiplication factor M is equal to unity. When only the holes are multiplied in the multiplication layer, the noise factor can be calculated according to the formula [15]:

$$F = M \left[1 - (1 - k_{ef}) \left(1 - \frac{1}{M} \right)^2 \right], \quad (2)$$

where k_{ef} is effective relation of electron and hole ionization factors. Noise factor dependence on carrier multiplication factor, when $k_{ef} = 0.45$, is presented in Fig. 8: experimental data well coincides with that calculated by formula (2).

3.3. Influence of the X-ray radiation

Ionizing radiation, similarly as thermal burn-in, can be used for the semiconductor structure parameter improvement and stabilization. In this section, examination of X-ray radiation influence to the avalanche photodiode operation characteristics, especially to the dark current and the $1/f$ noise level, is presented. Investigated APDs were irradiated by X-rays with dose power $3.4 \text{ Gy}/(\text{s}\cdot\text{cm}^2)$ and using accelerating voltage of 30 kV on Cu tube anticathode. Dark current, photocurrent, and noise characteristics have been measured after irradiation.

Dark current–voltage characteristics of initial APD and after APD irradiation for 30 min are presented in

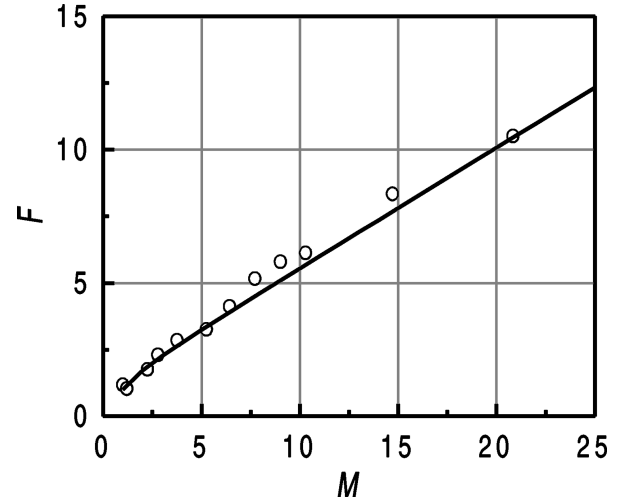


Fig. 8. APD shot noise factor dependence on the carrier multiplication factor (dots are experimental data, line is calculated by formula (2) with $k_{ef} = 0.45$).

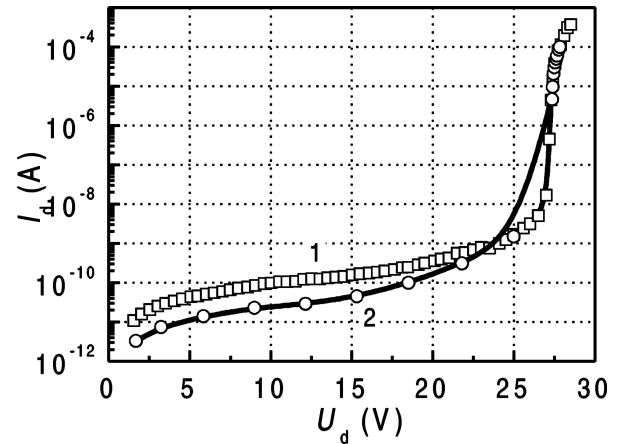


Fig. 9. APD dark current dependence on reverse voltage of initial sample (line 1) and after 30 min irradiation by X-rays (line 2); X-ray power $3.4 \text{ Gy}/(\text{s}\cdot\text{cm}^2)$.

Fig. 9. After irradiation the dark current at the reverse voltage below punch-through value decreased: at $U_d = 10 \text{ V}$ bias dark current decreased from 100 to 20 pA. The dark current reduction indicates that under X-ray radiation effective density of recombination centres decrease, i. e. the number of point defects in the device structure decreases. At larger reverse voltage the effect of X-ray radiation is less noticeable. And in avalanche breakdown region there is no dark current difference before and after irradiation. Photocurrent changes due to ionizing radiation are imperceptible.

The APD noise characteristic changes under X-ray irradiation are presented in Fig. 10. At low frequencies (below 1 kHz) the prevailing $1/f$ type noise was quite intensive in the initial sample noise spectra (graph (a) in Fig. 10): noise spectral density exceeded the value of

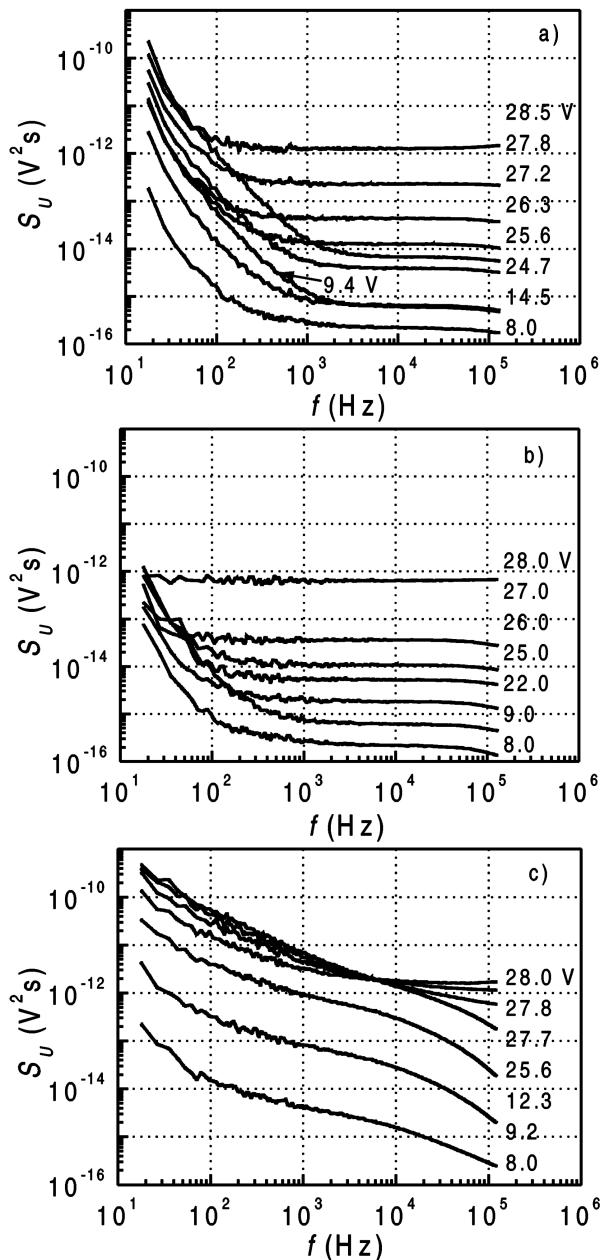


Fig. 10. APD noise spectra at different reverse voltages: (a) for initial sample, (b) after 30 min irradiation by ionizing radiation, (c) after the second 30 min irradiation (samples illuminated with HB, IR light power 10 μ W).

10^{-10} V²/s at 20 Hz. After 30 min X-ray irradiation the $1/f$ type noise intensity noticeably decreased: spectral density was lower than 10^{-12} V²/s at 20 Hz. The $1/f$ type noise intensity decrease confirms the dark current measurement results: the lower $1/f$ type noise level points to a lower number of active defects. Thereby, X-ray radiation acts similarly as burn-in process: significant part of unstable point defects vanish. Repeating dark current and noise measurements with a few days intervals, the further changes of APD character-

istics were not observed: achieved device parameters were stable.

After irradiated APD characteristic investigation, the same devices were irradiated by X-rays for the second 30 min period. As it is presented in graph (c) in Fig. 10, $1/f$ type noise intensity significantly increases after the second irradiation: noise spectral density at 20 Hz exceeds 10^{-10} V²/s value, and $1/f$ type fluctuations prevail over the shot noise up to 10 kHz. So, the second irradiation by X-rays creates active defects with wide distribution of relaxation times.

4. Conclusions

A detailed investigation of photoconductivity and noise characteristics of ultrafast InGaAs / InP avalanche photodiodes was carried out. The presented results have shown that noise characteristics clarify not only the fundamental physical processes that determine charge carrier transport and multiplication in avalanche photodiodes, but also the origin and changes of various defects during photodiode structure growth and device aging.

Terminal voltage fluctuations of avalanche photodiodes comprise the shot, generation-recombination, and $1/f$ type noise. At the reverse bias lower than punch-through voltage the shot and $1/f$ noises dominate. When carrier multiplication starts, shot multiplication noise level increases in the active area. In the periphery and at the active area interfaces the large generation-recombination fluctuations are observed. These generation-recombination fluctuations indicate a defective active area interface.

It is shown that the peripheral region of investigated avalanche photodiodes is also sensitive to the infrared radiation, and for the carrier multiplication factor evaluation the input light beam should be strongly focused to the spot not larger than the active area of photodiode or photodiode peripheral area must be covered with a light impenetrable layer.

It is also shown that an optimal (of certain dose and duration) one-time irradiation of avalanche photodiodes by X-rays decreases the number of active point defects in the structure and improves the device operation characteristics: it decreases the dark current and $1/f$ noise level.

Acknowledgements

This work has been partly funded by the Lithuanian State Science and Studies Foundation (contract No. C-33/2005/2006).

The authors would like to thank Bookham for providing APD device samples and to thank Stephen Jones, Richard Ash, and Robert Mallard for helpful discussions.

References

- [1] L.E. Tarof, Planar In/InGaAs avalanche photodetectors with gain-bandwidth product in excess of 100 GHz, *Electron. Lett.* **27**, 34–36 (1991).
- [2] L.E. Tarof, J. Yu, R. Bruce, D.G. Knight, T. Baird, and B. Oosterbrink, High frequency performance of separate absorption, grading, charge, and multiplication InP/InGaAs avalanche photodiodes, *IEEE Photon. Technol. Lett.* **5**, 672–674 (1993).
- [3] V. Palenskis, Flicker noise problem (review), *Lithuanian Phys. J.* **30**, 107–152 (1990).
- [4] B.K. Jones, Electrical noise as a measure of quality and reliability in electronic devices, *Adv. Electron. Electron. Phys.* **87**, 201–257 (1994).
- [5] J. Matukas, V. Palenskis, S. Pralgauskaite, and A. Vizbaras, Photosensitivity and noise characteristics investigation of ultrafast InGaAsP/InP avalanche photodetectors, in: *Proceedings of the XVI International Conference on Microwaves, Radar and Wireless Communications* (Krakow, 2006) pp. 173–176.
- [6] X. Zhao, M.J. Deen, and L. Tarof, Low-frequency noise in separate absorption, grading, charge and multiplication (SAGCM) avalanche photodiodes, *Electron Lett.* **32**, 250–252 (1996).
- [7] S. An and M.J. Deen, Low-frequency noise in single growth planar separate absorption, grading, charge and multiplication avalanche photodiodes, *IEEE Trans. Electron. Devices* **47**, 537–543 (2000).
- [8] R.J. McIntyre, Multiplication noise in uniform avalanche diodes, *IEEE Trans. Electron. Devices* **13**, 164–168 (1966).
- [9] R.J. McIntyre, The distribution of gains in uniformly multiplying avalanche diodes: Theory, *IEEE Trans. Electron. Devices* **19**, 703–713 (1972).
- [10] R.J. McIntyre, A new look at impact ionization – Part I: A theory of gain, noise, breakdown probability, and frequency response, *IEEE Trans. Electron. Devices* **46**, 1623–1631 (1999).
- [11] P. Yuan, K.A. Anselm, C. Hu, H. Nie, C. Lenox, A.L. Holmes, B.G. Streetman, J.C. Campbell, and R.J. McIntyre, A new look at impact ionization – Part II: Gain and noise in short avalanche diodes, *IEEE Trans. Electron. Devices* **46**, 1632–1639 (1999).
- [12] T. Takanohashi, T. Shirai, S. Yamazaki, S. Komiya, and I. Umebu, Inhomogeneous distribution of avalanche multiplication on InP APDs, *Japan J. Appl. Phys.* **23**, 270–271 (1984).
- [13] N. Magnea, P.M. Petroff, F. Capasso, R.A. Logan, and P.W. Foy, Microplasma characteristics in LPE grown InP–In_{0.53}Ga_{0.47} long wavelength avalanche photodiodes with separated multiplication and absorption regions, *Appl. Phys. Lett.* **46**, 1074–1076 (1985).
- [14] V. Palenskis, J. Matukas, D. Stučinskas, K.A. Kaminskis, and E. Žitkevičius, Investigation of noise in InGaAs/InP-based separate absorption and multiplication avalanche photodiodes, *Lithuanian J. Phys.* **45**, 385–390 (2003).
- [15] Y.K. Jhee, J.C. Campbell, W.S. Holden, A.G. Dental, and J.K. Plourde, The effect of nonuniform gain on the multiplication noise of InP/InGaAsP/InGaAs, *IEEE J. Quantum Electron.* **21**, 1858–1861 (1985).

YPAČ SPARČIŲ InGaAs/InP GRIŪTINIŲ FOTODIODŲ FOTOJAUTRIS IR TRIUKŠMAI

J. Matukas, V. Palenskis, S. Pralgauskaitė, R. Gadonas, R. Purlys, A. Čiburys, A. Vizbaras

*Vilniaus universitetas, Vilnius, Lietuva***Santrauka**

Atlikti sparčių InGaAs/InP griūtinių fotodiodų su atskiromis sugerties ir krūvininkų dauginimo sritimis fotojautrio ir triukšmo charakteristikų tyrimai, įvertinti krūvininkų dauginimo ir triukšmo faktoriai. Taip pat ištirtas jonizuojančios spinduliuotės poveikis griūtinių fotodiodų charakteristikoms.

Nustatyta, kad tirtųjų fotodiodų paviršiaus periferinė sritis yra jautri infraraudonajai spinduliuotei, todėl krūvininkų dauginimo ir triukšmo faktoriai teisingai įvertinami tik tada, kai apšviečiama tik aktyvioji sritis – krentanti spinduliuotė turi būti sufokusuota į dėmę, ne didesnę nei aktyviosios srities matmenys. Eksperimentinė triukšmo faktoriaus priklausomybė nuo krūvininkų dauginimo faktoriaus sutampa su teorine, kai efektyvusis elektronų ir skylių jonizacijos faktorių santykis $k_{\text{ef}} = 0,45$.

Griūtinių fotodiodų įtampos fliktuacijas lemia šratinio, generacinio-rekombinacinio ir $1/f$ triukšmo superpozicija. Kol atgalinė

įtampa neviršija pradūros įtampos, vyrauja šratinis ir $1/f$ triukšmas. Prasidėjus griūtiniam krūvininkų dauginimui, aktyviojoje srityje išauga šratinio triukšmo lygis. Periferinėje srityje bei aktyviosios srities riboje su periferine sritimi stebimas intensyvus generacinis-rekombinacinis triukšmas.

Tam tikrą laiką tarpą švitinant fotodiodą tam tikros galios Rentgeno spinduliuote, sumažėja defektų skaičių darinyje – pagerėja fotodiodo charakteristikos: sumažėja tamsinė srovė bei $1/f$ triukšmo intensyvumas. Tačiau per ilgai arba pakartotinai švitinant fotodiodus, defektų tankis padidėja, fotodiodo charakteristikos pablogėja. Triukšmo charakteristikų tyrimai ne tik atskleidžia fundamentinius fizikinius vyksmus, nulemiančius krūvininkų pernašą bei dauginimą griūtinio fotodiodo darinyje, bet taip pat leidžia įvertinti įvairių defektų buvimą bei jų kitimą fotodiodo darinyje, jų įtaką fotodiodo kokybei bei senėjimo procesams.